ORNL/CP-98579

CONF-980668--

MML '98 3rd International Symposium on Metallic Multilayers,
Vancouver, Canada, June, 1998

THE ROLE OF CR ANTIFERROMAGNETISM ON INTERLAYER MAGNETIC COUPLING IN FE/CR MULTILAYERED SYSTEMS

Z.-P. Shi and R. S. Fishman

SOLID STATE DIVISION
OAK RIDGE NATIONAL LABORATORY
Managed by
LOCKHEED MARTIN ENERGY RESEARCH CORP.
Under
Contract No. DE-AC05-96OR22464
With the
U. S. DEPARTMENT OF ENERGY
OAK RIDGE, TENNESSEE

June 1998

DISTRIBUTION OF THIS DOCUMENT IS UNLIMITED

DISCLAIMER

DISCLAIMER

Portions of this document may be illegible in electronic image products. Images are produced from the best available original document.

The Role of Cr Antiferromagnetism on Interlayer Magnetic Coupling in Fe/Cr Multilayered Systems

Zhu-Pei Shi
R & D Division, Read-Rite Corporation, 44100 Osgood Road, Fremont, CA 94539
R. S. Fishman
Solid State Division, Oak Ridge National Laboratory, Oak Ridge, TN 37831-6032

Abstract
Many experiments have verified the presence of a spin-density wave (SDW) within the Cr spacer of Fe/Cr multilayers and wedges. We review the recently-proposed interlayer magnetic coupling mediated by a SDW. Unlike previously proposed mechanisms, this magnetic coupling is strongly temperature-dependent. Depending on the temperature and the number **N** of Cr monolayers (ML), the SDW may be either commensurate (C) or incommensurate (I) with the bcc Cr lattice.

I Introduction -

There is a great deal of current interest in the properties of magnetic multilayered structures consisting of alternating thin ferromagnetic and non-ferromagnetic metallic layers. The antiferromagnetic coupling first observed between the Fe layers separated by a thin Cr spacer [1] and the giant magnetoresistance (GMR) found in this system [2] have led to intense theoretical and experimental studies of an extraordinary range of structures over the past few years. In metallic magnetic layers, the magnitude of the GMR effect oscillates as the thickness of the non-ferromagnetic spacer layers is increased [3]. This oscillation is associated with an oscillation in the sign (ferro- or antiferro-magnetic) of the interlayer magnetic coupling between the ferromagnetic layers.

Oscillatory interlayer coupling is known to be a very general property of almost all transition-metal magnetic multilayered systems in which the non-ferromagnetic layer comprises one of the 3d, 4d, or 5d transition metals or one of the noble metals. This oscillatory behavior can be explained by applying the general exchange theory of Ruderman-Kittel-Kasuya-Yosida (RKKY) to the problem of the interlayer coupling [4]. This theory provides a physically transparent explanation of the measured oscillatory periods in terms of the topological properties of the spacer Fermi surface. It is now well accepted that interlayer coupling between separated magnetic layers occurs because of the spin polarization of the intervening conduction electrons and the associated magnetic scattering of conduction electrons with their moments in the magnetic layer. But even after intensive studies of interlayer magnetic coupling [5], Fe/Cr heterostructures have continued to surprise scientists with their unique properties.

Due to the competition between the SDW ordering in the Cr spacer [6] and the Fe-Cr interactions at the interfaces, Fe/Cr multilayers and wedges have provided new insight into the physics of transition-metal magnets. Depending on temperature and spacer thickness, the SDW may be either commensurate or incommensurate with the bcc Cr lattice. For

Fe/Cr multilayers [7], the C SDW phase is stabilized when the number of monolayers N inside the Cr spacer is less than 30 or when the temperature exceeds the Neel temperature 310 K of pure Cr. By contrast, SEMPA measurements [8] on Fe/Cr/Fe wedges indicate that the I SDW phase is stable for $N >$ 23 ML's and up to at least 550 K. As the spacer thickness increases, the Fe-Fe coupling alternates between ferromagnetic (F) and antiferromagnet (AF) with phase slips every 20 ML's at room temperature. Here we review a new type of exchange mechanism in which the coupling between ferromagnetic layers is mediated by the SDW of the Cr spacer [9].

The organization of the paper is as follows. Section II provides the general formalism of interlayer magnetic coupling mediated by a SDW. As shown in Section III, this coupling is strongly temperature-dependent. Section IV describes the I-to-C SDW transition in the Cr spacers. Section V illustrates the stretching and relaxing cycle of the SDW as the spacer thickness is increased. Possible effect of interface roughness on the SDW ordering and Neel temperature are addressed in Section VI. Section VII contains some final remarks.

II Interlayer Coupling Mediated by Spin-Density Waves

Interlayer magnetic coupling across noble metal spacers can be well understood in terms of the RKKY coupling mechanism and the oscillation periods can be accurately determined by ab initio calculations [5]. The interlayer coupling in Fe/Cr/Fe multilayers, however, show some unusual features such as an antiferromagnetic bias at ultra thin Cr spacer and strong temperature dependence [10]. Shi et al [11] proposed a coupling mechanism based on the s-d mixing interactions at Fe/Cr interfaces. The RKKY oscillatory terms are superposed upon an antiferromagnetic background in order to interpret the interlayer magnetic coupling in Fe/Cr multilayers. However, the SDW ordering observed in Fe/Cr multilayers [7-8] and the strongly temperature-dependent interlayer coupling challenge all RKKY-like coupling mechanisms and zero-temperature ab initio calculations. The SDW-mediated coupling [9] reviewed here provides a new theoretical framework to address the unusual magnetic properties observed in Fe/Cr systems.

The SDW instability in Cr alloys is produced by the Coulomb attraction between electrons and holes on nearly perfectly nested electron and hole Fermi surfaces, both roughly octahedral in shape [4]. Because the electron Fermi surface is slightly smaller than the hole Fermi surface, there are two different nesting wavevectors $Q_{\pm}$ which translate four faces of one Fermi surface onto four faces of the other. The nesting wavevectors may be written as $Q_{\pm} = 2\pi/a(1 \pm \delta)$, where $\delta \sim 0.05$ is a measure of the size difference between the electron and hole Fermi surfaces, and a is the bcc lattice constant. Unlike the condensate of a superconductor, which contains pairs of electrons with zero total momentum, the condensate of an I SDW contains pairs of electrons and holes with nonzero total momentum. In the I phase of the SDW, the condensate contains two types of electron-hole pairs with momenta $Q'_{\pm} = 2\pi/a(1 \pm \delta')$. When $\delta'=0$, the SDW is commensurate with underlying lattice. If the SDW wave vector lies along the z direction normal to the multilayer interface, the spin at each atomic layer can be written

$$S(z) = \hat{m}\alpha_s g(-1)^{2z/a}\cos[\frac{2\pi}{a}\delta' z - \theta)], \quad (1)$$

where α_s is a constant, θ is an arbitrary phase, g is an order parameter, and $\alpha_s g$=0.6μ_B for bulk Cr at zero temperature.

For simplicity, we assume that the Fe moments are either F or AF aligned with S^I_{Fe}= S^{II}_{Fe} or S^I_{Fe}= -S^{II}_{Fe}, both parallel to the interface. The SDW will then be transversely polarized with respect to the ordering wave vectors along the z axis. With antiferromagnetic interactions at the interfaces [12], the total energy of the multilayer or wedge for an interfacial area of a^2 and spacer width $(N-1)a/2$ may be written as [9]

$$E = AS^I_{Fe} \bullet S(1) + AS^{II}_{Fe} \bullet S(N) + \Delta F a^3 (N-1)/2, \quad (2)$$

which assumes that the SDW is rigid with order parameters g and δ' independent of z. Here ΔF is the free energy of the SDW phases in Cr spacer. It is a function of g, δ', T, and energy mismatch ε_0 between the electron and hole Fermi surfaces [9].

After fixing the magnetic configurations of the Fe layers, the SDW order parameters g and δ' as well as the arbitrary phase θ are chosen to minimize the energy E in Eq. (2). The corresponding F and AF energies of the trilayer are

$$E_F = -2A\alpha_s g S_{Fe}|\cos\phi| + \Delta F(g,\Lambda,T,\varepsilon_0)a^3(N-1)/2, \quad (3)$$

$$E_{AF} = -2A\alpha_s g S_{Fe}|\sin\phi| + \Delta F(g,\Lambda,T,\varepsilon_0)a^3(N-1)/2, \quad (4)$$

where $\phi=(\pi/2)(N-1)(1+\delta')$. The SDW order parameter is restricted to values below the bulk maximum of $g_{max}=1.246\ T_N^*$, which is achieved in the C SDW phase of a bulk Cr alloy at $T=0$ (T_N^*~80meV).

Because the nesting free energy ΔF is proportional to $\rho_{eh}\ T_N^{*2}$, the total free energy E depends only on the dimensionless constant

$$\gamma = \frac{A\alpha_s S_{Fe}}{(V/N)\rho_{eh} T_N^*}, \quad (5)$$

which represents the average coupling strength between Fe and Cr at the interfaces. It can be estimated either from first-principles calculations or by comparison with the experimental data.

Once E_{AF} and E_F are found, the magnetic coupling $J_{coup} = E_{AF} - E_F$ may be evaluated as a function of temperature T and spacer thickness N.

III Strongly Temperature-Dependent Magnetic Coupling

Taking $\gamma=1$, $\varepsilon_0/T_N^*=5$, and $T=0.5T_N$ or $1.2T_N$, we plot J_{coup} as a function of spacer thickness in Fig. 1. As expected, J_{coup} oscillates between F (>0) and AF (<0) values with a short 2 ML period. As shown in Fig.1(a), above the Neel temperature, the magnetic coupling falls off rapidly with the size of the spacer. For large N, we show in Ref. 13 that J_{coup} decreases like $1/N^2$. So above T_N, the RKKY and nesting contributions to the magnetic coupling cannot be distinguished by their dependence on N. Below the Neel

temperature, the magnetic coupling decays slowly with the size of the spacer as shown in Fig. 1(b). J_{coup} falls off like $1/N^{0.5}$ below T_N [13]. This decay is slower than indicated by either a Kohn-anomaly analysis ($J_{coup} \sim 1/N$) [14] or density-functional total energy calculations ($J_{coup} \sim 1/N^{1.25}$ at $T = 0$ [15]).

Fixing the thickness of the spacer, we evaluate the magnetic coupling as a function of temperature. For $N=25$ and $\gamma=1$ and $T=0.5T_N$, J_{coup} is plotted as the solid curve in Fig. 2. Notice that antiferromagnetic coupling at low temperature decreases by a factor of 2 as the temperature increases to T_N, and becomes weakly ferromagnetic coupling above $1.41T_N$. Because the temperature is much less than the Fermi energy, the conventional RKKY coupling mediated by spin-polarized electronic states is only weakly temperature-dependent [16]. At least qualitatively, our model explains the rapid decrease in the coupling strength of Fe/Cr multilayers above T_N [10] and the disappearance of the AF coupling above 320 K in Co/Mn multilayers [17].

IV Incommensurate to Commensurate SDW Transitions in Cr Spacers

For $N=25$, $\gamma=1$, and $T=0.5T_N$, the energies of F and AF magnetic configurations are individually plotted as dashed and dotted curves. The solid dot on the F curve indicates an I-to-C SDW transition in the Cr spacers. This prediction [9] has been confirmed by recent neutron scattering measurements of Fe/Cr multilayers [18].

The proximity Fe layers will modify the SDW order parameters of the Cr spacer. In the absence of interface coupling ($\gamma=0$), the bulk values of the SDW amplitude g and wave vector δ' are evaluated by minimizing ΔF [9]. If $T=0.5T_N$, then $g_{bulk}=0.647T_N^*$ and $\delta'_{bulk}=0.0378$. When $\gamma>0$, the SDW order parameter g always exceeds its bulk value. After fixing the magnetic configurations of the proximity magnetic layers, we found that both order parameters oscillate as a function of the spacer thickness with a 2 ML period and approach their bulk values as N goes to infinity. For F arranged Fe layers with $T=0.5T_N$ and $\gamma=2.5$, δ' is given by the dotted line in Fig. 3. For AF arranged magnetic layers, the oscillation patterns of δ' plotted in Fig. 3 are shifted to the right by one ML (with the same shift for the SDW order parameter g). The order parameter δ' corresponding to the lowest energy magnetic configurations (F or AF) of the proximity Fe layers is also plotted in Fig. 3, a thick solid curve. So for N between 24 and 39, the F (AF) configurations are stable for even (odd) N while for N between 40 and 61, F (AF) configurations are stable for odd (even) N. The order parameter g has the same behavior as that of δ'. The steps on the stable line of the order parameters at the spacer thickness of 23, 39, and 61 ML correspond to the nodes of J_{coup} [9]. The first step on the "stable line" in Fig. 3 agrees with recent neutron scattering measurements [7], where a C-to-I SDW transition between 21 and 35 ML is observed. The other steps on the "stable line" stand for I-to-I SDW phase transitions which are clearly indicated by the NIST measurements [8].

V Stretching and Relaxing Cycle of SDW in Cr Spacers

While the SDW order parameters g and δ' jump between lower and higher values with a period of *2* ML, their oscillation patterns shift at spacer thicknesses of *34*, *51*, and *74* ML, as shown in Fig. 3. This striking behavior can be explained by the competition between the interface coupling, which maximizes the SDW amplitude at the boundaries, and the intrinsic antiferromagnetism of the Cr spacer, which favors the bulk values of the SDW amplitude and wave vector. As the Cr spacer thickness increases for odd or even N in Fig. 3, the SDW first stretches to optimize the interface coupling and then suddenly relaxes to lower the bulk free energy. For example, the SDW with $N=34$ ML drawn as the solid curve in Fig. 4 contains a single node. As even N increases, the SDW stretches until it attains the profile of the dotted curve for $N=50$ ML. With the addition of two more ML's, two new nodes appear in the SDW (dashed curve) and the SDW amplitude drops towards its bulk value. As N increases further, the cycle of stretching and relaxing repeats with a period close to the wavelength ~*40* ML of the bulk SDW. For odd N, the same cycle is offset by about *20* ML. So the jumps in the SDW order parameters at *34*, *51*, and *74* ML are also separated by about *20* ML.

VI Oscillatory Neel Temperature in Fe/Cr Systems

Sputtered Fe/Cr multilayers may have thickness fluctuations or atomic steps at the interfaces. Such fluctuations may establish the SDW nodes near the interfaces [7], in which case the Fe moments within the multilayers are not magnetically coupled. Assuming that the SDW nodes lie precisely at the Fe-Cr interfaces, δ' is restricted to the values $\delta'_n = (n-1)/(N-1)$, where $n \geq 2$ is the number of SDW nodes including the two at the interfaces [19]. We evaluate n by minimizing the nesting free energy $\Delta F(g, \delta'_n)$ with respect to both g and n.

Because the C SDW does not contain any nodes, the C SDW phase is never stabilized in this case. In Fig.5, the Neel temperature T_N and phase boundaries are normalized by the bulk Neel temperature $T_{N,bulk}$, which is evaluated by allowing δ' to be a continuous parameter. Here we take $\varepsilon_0=5T^*_N$ and $\delta = 0.043$. So the bulk value of δ' at $T_{N,bulk}$ is 0.037, corresponding to a node-to-node distance of 27 ML's. For $T/T_{N,bulk}=0.2$, the SDW order parameter δ' are plotted versus N in Fig. 6. As N decreases below *41* ML's, δ' increases and the SDW period decreases as a half-wavelength of the SDW tries to squeeze into the Cr spacer. When $N < 27$, δ' is larger than its bulk value so that the SDW period is smaller than in bulk. For $N< 20$ ML's, a half-wavelength of the SDW cannot squeeze into the Cr spacer without a prohibitive cost in free energy and the Neel temperature drops to zero. As N increases, the SDW goes through cycles of expansions followed by sudden contractions with the addition of another node to the SDW. As δ' plotted in Fig. 6 decreases, the amplitude g grows. In other words, the cyclical expansion and contraction of the SDW follows the same pattern as depicted by Fig. 3. Only now these cycles also produce an oscillatory pattern in T_N. Whenever δ' passes near the bulk value of 0.037, T_N reaches a maximum.

The measurements by Fullerton *et al.* [7] provide some evidence for this behavior. Fits to their data reveal that the SDW nodes lie very close to the Fe-Cr interfaces *except* for $N=35$, corresponding to a SDW with $n=2$ near the predicted depression in T_N. For this SDW, Fullerton *et al.* find that the antinodes rather than the nodes lie close to the Fe-Cr interfaces. However, their data for $N=35$ can be equally well described by a SDW with nodes displaced 7 ML's from each interface.

VII Conclusions

Based on a simple model with antiferromagmetic interactions at the Cr-Fe interfaces, the role of Cr antiferromagnetism on the exchange coupling and magnetic phase diagram of Fe/Cr multilayers has been reviewed. A SDW mediates a new type of interlayer magnetic coupling which is strongly temperature-dependent. The properties of this coupling are quite different from the well-known RKKY coupling. The Cr spacer undergoes a magnetic phase transition from an I to a C SDW below a critical spacer thickness or at high temperatures. These theoretical results agree with recent polarized neutron scattering measurements.

One of authors (RSF) was supported by Oak Ridge National Laboratory managed by Lockheed Martin Energy Research Corp. for the U.S. Department of Energy under Contract No. DE-AC05-96OR22464.

References

[1] P. Grunberg, R. Schreiber, Y. Pang, M. B. Brodsky, and H. Sowers, Phys. Rev. Lett. **57**, 2442 (1986).

[2] M.N. Baibich, J.M. Broto, A. Fert, F. Nguyen Van Dau, F. Petroff, P. Eitenne, G. Creuzet, A, Friederich, and J. Chazelas , Phys. Rev. Lett. **61**, 2472 (1988).

[3] S.S. P. Parkin, N. More, and K. P. Roche, Phys. Rev. Lett. **67**, 3598 (1991).

[4] P. Bruno and C. Chappert, Phys. Rev. Lett. **67**, 1602 (1991).

[5] For a review, see for an example, B. Heinrich and J. F. Cochran, Advances in Physics, **42**, 523 (1993).

[6] E. Fawcett, Rev. Mod. Phys. **60**, 209 (1988); E. Fawcett *et al.*, Rev. Mod. Phys. **66**, 25 (1994).

[7]E. E. Fullerton, S. D. Bader, and J. L. Robertson, Phys. Rev. Lett. **77**, 1382 (1996).

[8] J. Unguris, R.J. Celotta, and D.T. Pierce, Phys. Rev. Lett. **67**, 140 (1991); **69**, 1125 (1992).

[9] Z. P. Shi and R. S. Fishman, Phys. Rev. Lett. **78**, 1351 (1997); R. S. Fishman and Z. P. Shi, J. Phys.: Cond. Matt. **10**, L277 (1998).

[10] E. E. Fullerton, J. E. Mattson, C. H. Sowers, and S. D. Bader, Scr. Metall. Mater. **33**, 1637 (1995).

[11] Z. P. Shi, P. M. Levy, and J. L. Fry, Phys. Rev. Lett. **69**, 3678 (1992); Europhys. Lett. **26**, 473 (1994).

[12] T. G. Walker, A. W. Pang, H. Hopster, and S. F. Alvarado, Phys. Rev. Lett. **69**, 1121 (1992).

[13] R. S. Fishman and Zhu-Pei Shi, Phys. Rev. B, to be published.

[14] D. D. Koelling, Phys. Rev. B **50**, 273 (1994).

[15] M. van Schilfgaarde, F. Herman, S. S. P. Parkin, J. Kudrnovsky, Phys. Rev. Lett. **74**, 4063 (1995).

[16] Z. Zhang, L. Zhou, P. E. Wigen, and K. Ounadjela, Phys. Rev. Lett.**73**, 336 (1994).

[17] Y. Henry and K. Ounadjela, Phys. Rev. Lett. **76**, 1944 (1996).

[18] A. Schreyer *et al*, Phys. Rev. Lett. **79**, 4914 (1997).

[19] R. S. Fishman, Phys. Rev. B **57**, 10284 (1998).

FIGURE CAPTIONS

Fig. 1 Bilinear magnetic coupling as a function of spacer thickness for $\gamma=1$ and (a) $T=0.5T_N$ or (b) $T=1.2T_N$.

Fig. 2 Magnetic energies as functions of temperature for $\gamma=1$ and $N=25$ ML. The solid dot denotes the I-to-C transition for a SDW with F coupling.

Fig.3 SDW wave vector parameter δ' as a function of spacer thickness for $T=0.5T_N$ and $\gamma=2.5$. The dotted line is for F arranged magnetic layers and the solid line is for the stable magnetic configuration (F or AF) with the lowest energy.

Fig. 4 SDW profiles in the spacer for $N=34$ (solid), 50 (dotted), and 52 (dashed) for the same parameters as in Fig. 3.

Fig. 5 Neel temperature versus N. The number of SDW nodes is given by n.

Fig. 6 SDW wave vector versus N for $T/T_{N,bulk}=0.2$. The bulk values are indicated by the dashed lines.

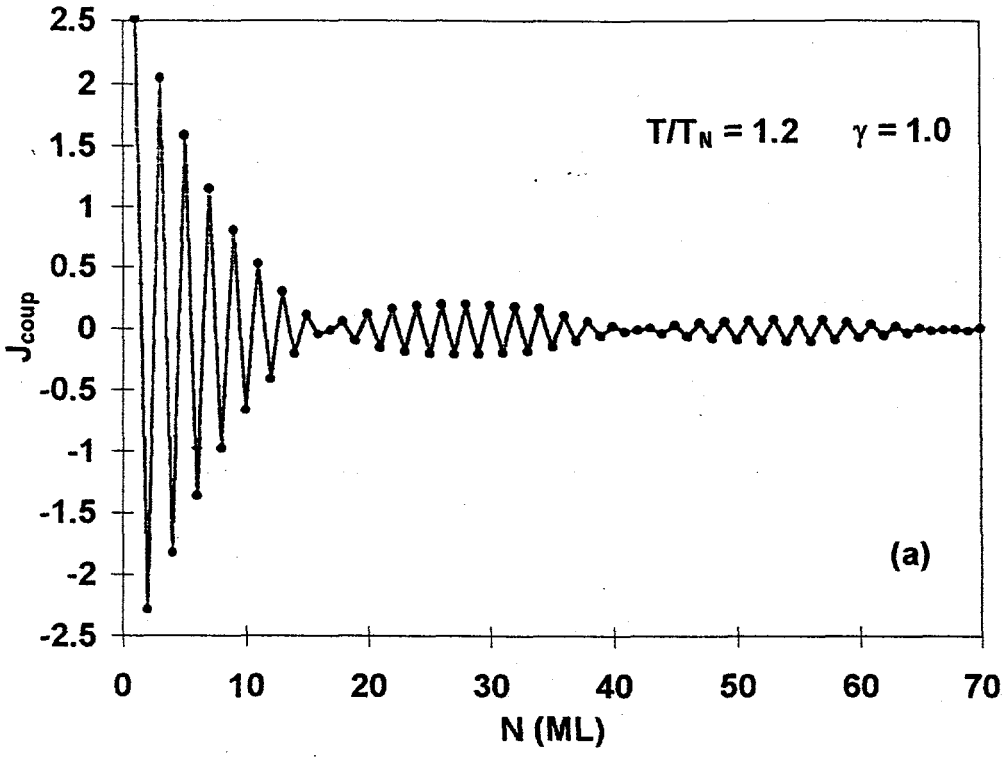

Fig. 1(a)

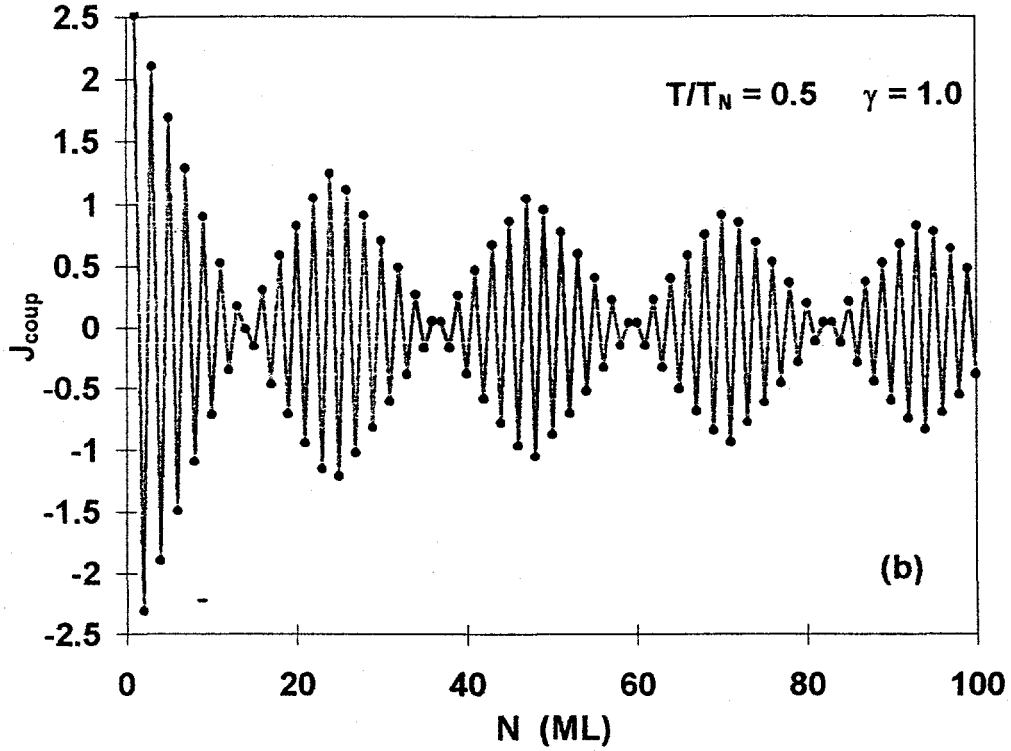
2.5
2
1.5
1
0.5
0
-0.5
-1
-1.5
-2
-2.5
J_{coup}
$T/T_N = 0.5$ $\gamma = 1.0$
(b)
0
20
40
60
80
100
N (ML)

Fig. 1(b)

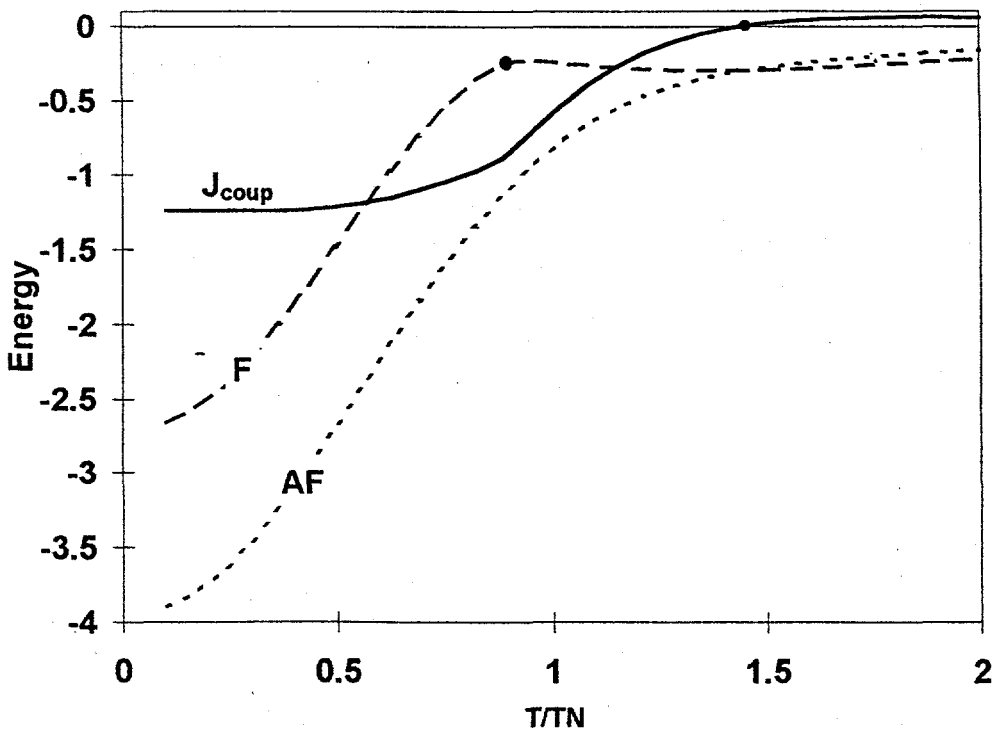
0
-0.5
-1
-1.5
-2
-2.5
-3
-3.5
-4
Energy
J_{coup}
F
AF
0
0.5
1
1.5
2
T/TN

Fig. 2

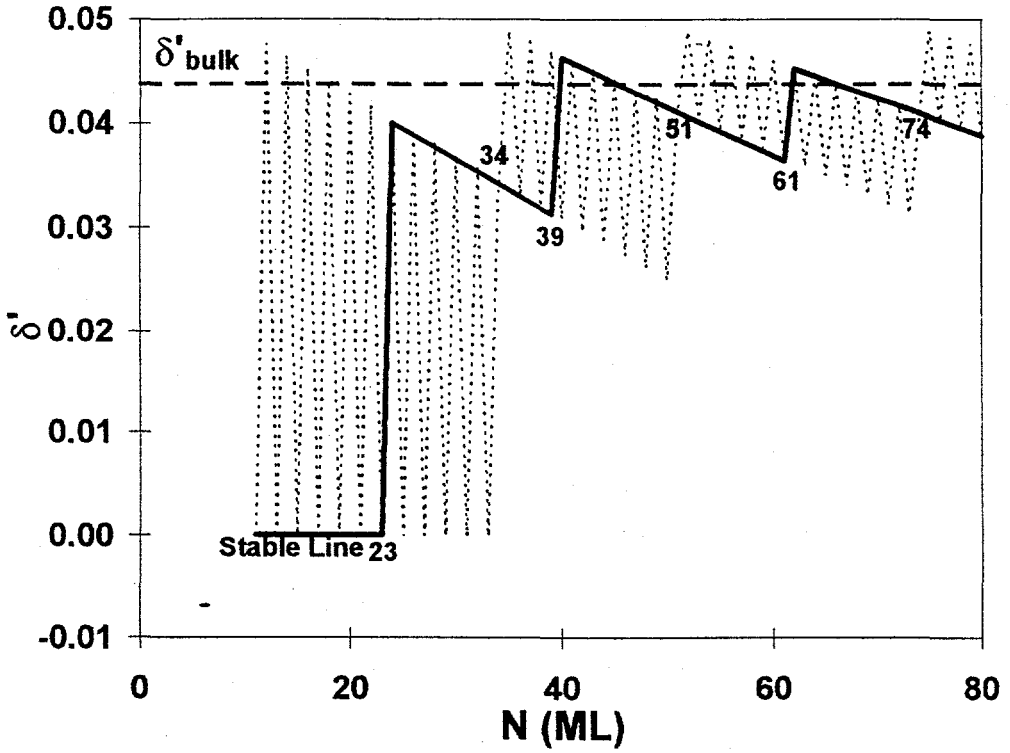
0.05
0.04
0.03
0.02
0.01
0.00
-0.01
δ'
δ'bulk
34
39
51
61
74
Stable Line 23
0
20
40
60
80
N (ML)

Fig.3

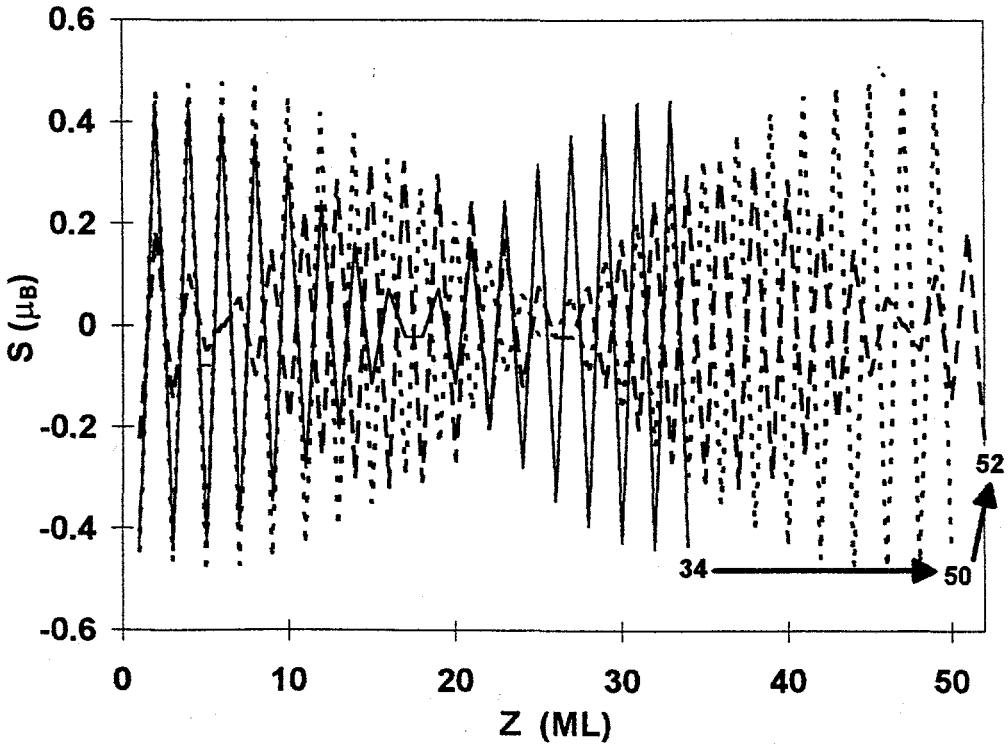
0.6
0.4
0.2
0
-0.2
-0.4
-0.6
S (μB)
52
34
50
0
10
20
30
40
50
Z (ML)

Fig. 4

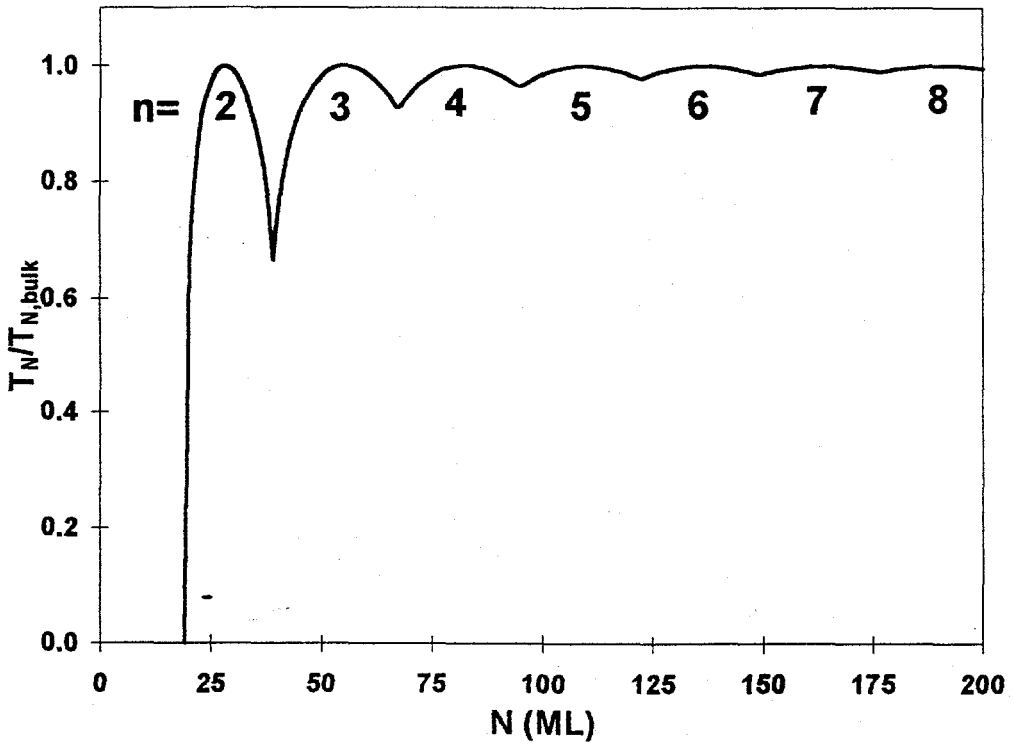
n=
2
3
4
5
6
7
8
1.0
0.8
0.6
0.4
0.2
0.0
$T_N/T_{N,bulk}$
0
25
50
75
100
125
150
175
200
N (ML)

Fig.5

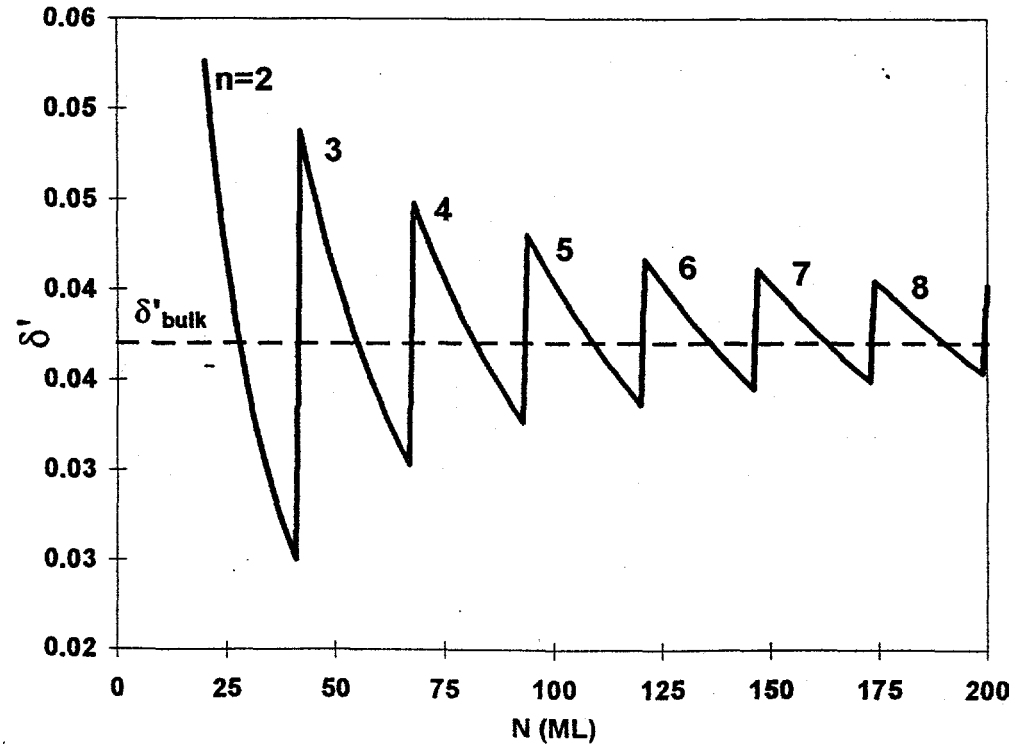
n=2
3
4
5
6
7
8
δ'_{bulk}
0.06
0.05
0.05
0.04
0.04
0.03
0.03
0.02
δ'
0
25
50
75
100
125
150
175
200
N (ML)

Fig.6